

A Numerical Study of Non-local Magneto Transport Effects in Quantum Hall Device Structures

Josef Oswald, Christoph Uiberacker, Christian Stecher

Institute for Physics, University of Leoben, Franz Josef Str. 18, A-8700 Leoben, Austria

E-mail: `josef.oswald@unileoben.ac.at`

Abstract. We developed a non-equilibrium network model for magneto transport in 2D electronic systems in the quantum Hall effect regime, which is able to capture the real sample geometry, including contacts, leads and in-homogeneities like introduced by gate electrodes. In this paper we investigate non-local effects in magneto transport for a number of contact configurations of a quantum Hall system, including the effect of having unused metallic contacts between the active region of classical current flow and the remote region where the non-local signals are obtained.

1. Introduction

There are an increasing number of devices like applications of quantum Hall systems for various purposes. One is spintronics in context with injection and detection of spin polarized electrons, but there are also other device concepts like electron interferometers or terahertz emitters, which make use of the unique properties of edge states[1]. While theoretical approaches mostly rely on the equilibrium situation, experiments drive the system out of equilibrium so that in real experiments one always measures non-equilibrium currents and potentials. Especially non-local effects are driven by the presence of a non-equilibrium between bulk and edge channels (EC). An appropriate transport model should take care of this and has also to provide a link between the microscopic physics and the experimental answer of the finally macroscopic sample. We developed a non-equilibrium network model for magneto transport in 2D electronic systems in the quantum Hall effect regime, which is able to capture the real sample geometry, including contacts, leads and in-homogeneities like introduced by gate electrodes [2, 3, 4, 5, 6]. In this paper we are going to demonstrate, that also non-local effects can be addressed successfully.

2. The non-equilibrium network model

The intention of our network approach to magneto transport is to address directly the non-equilibrium current flow. This means that we have to deal with the situation of a non-uniform lateral distribution of the chemical potentials. We use a network of directed quantum channels, which interconnect a 2-dimensional arrangement of nodes, which physically correspond to the saddles of the potential fluctuations in real systems. The directed channels keep their chemical potentials between the nodes, while the nodes transmit and modify the chemical potentials from the incoming to the outgoing channels. The main facts are given below and for further details refer to the cited papers.[7, 8].

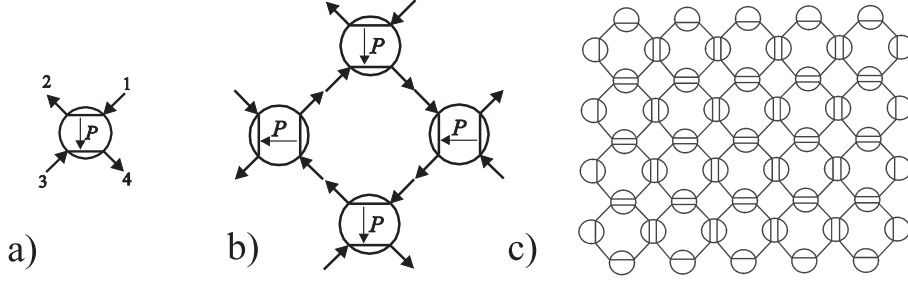


Figure 1. a) Node of the network with two incoming and two outgoing channels. The channels $1 \rightarrow 2$ and $3 \rightarrow 4$ are treated like ECs with back scattering, where $P = R/T$ corresponds to the relation between reflection and transmission coefficients according to the Landauer- Büttiker formalism. b) Arrangement of the nodes for building the minimal physical element of a network, which is the closed loop of a so called magnetic bound state. c) The complete network is composed by putting together a sufficient number of such adjacent loops.

Fig.1a shows a single node of our network, which transmits potentials from the incoming to the outgoing channels, Figs.1b-c demonstrate, how the network is composed. The potentials transmitted by one node are calculated by using $u_2 = (u_1 + P \cdot u_3)/(1 + P)$ and $u_4 = (u_3 + P \cdot u_1)/(1 + P)$. We attribute the non-equilibrium currents to channel pairs, like e.g. the current from the right to the left $I = (e^2/h) \cdot (u_1 - u_4)$ (see Fig.1a). It is important, that in this way our nodes provide a handle to both, the injected currents and the potentials. P results from tunneling across saddle points of the potential landscape in the bulk[7]: $P = \exp \left[-\frac{L^2 E_F}{eV} \frac{eB}{h} \right]$, E_F is the Fermi energy relative to the saddle energy which corresponds to the center of the LL, eB/h is the number of LL states, L is the period and \tilde{V} the amplitude of a representative two-dimensional Cosine-potential modulation, which has the same Taylor expansion like the actual saddle potential. Therefore the ratio L^2/\tilde{V} can be understood as a measure of the "smoothness" of the potential modulation near the saddle. The design of the sample is done by shaping the lateral confining bare potential and using a self consistent Hartree type approximation to calculate the Fermi energy and the lateral carrier distribution. On this basis a gate electrode can be easily modeled by biasing the bare potential of the designated gate region (for further details see cited papers).

3. Results and Discussion

For the numerical study we used a Hall bar with contact leads and also a more simple rectangular Hall conductor with point contacts at the edges, both with a bulk carrier density of $4 \cdot 10^{11} \text{ cm}^{-2}$. Fig.2 shows the simulations for the Hall bar structure. The current injection is done in an unusual fashion like indicated in the insert of Fig.2 on the left: One current contact at one end of the Hall bar is used as usual, but the other current contact is applied across the bulk at about half length of the Hall bar. The width of that contact stripe is chosen that it just touches the edge region, where the side depletion starts to develop. For geometry reasons there should be no signal at the remote (Hall) contact pair. As can be seen on the left of Fig.2, already at low fields there comes up a small non-local resistance which forms a kind of maximum at about $B=0.5$ Tesla, before Schubnikow-de-Haas oscillations set-in. In the high magnetic field regime on the right, a strong non-local signal develops, which appears like the longitudinal resistance in the QHE regime. The main reason for that is the introduced non-equilibrium between edge and bulk, while the symmetry of the sample is destroyed by the opposite directed ECs, which pass the interior current injection contact.

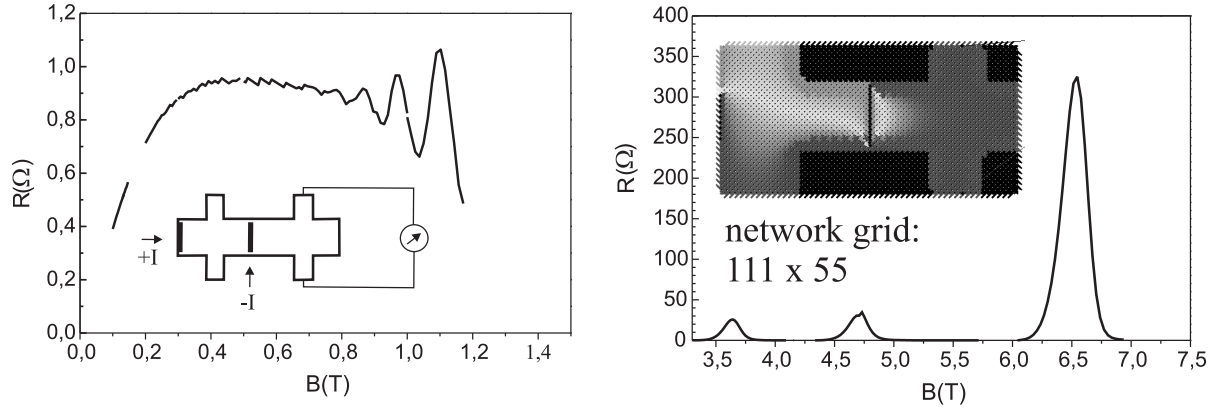


Figure 2. Left: Low field non-local resistance of a Hall bar. Insert: Contact scheme. Right: High field non-local resistance according to the contact scheme on the left. Insert: Screen shot of network layout. The gray scale inside the Hall bar represents the lateral distribution of the excitation potential (not discussed).

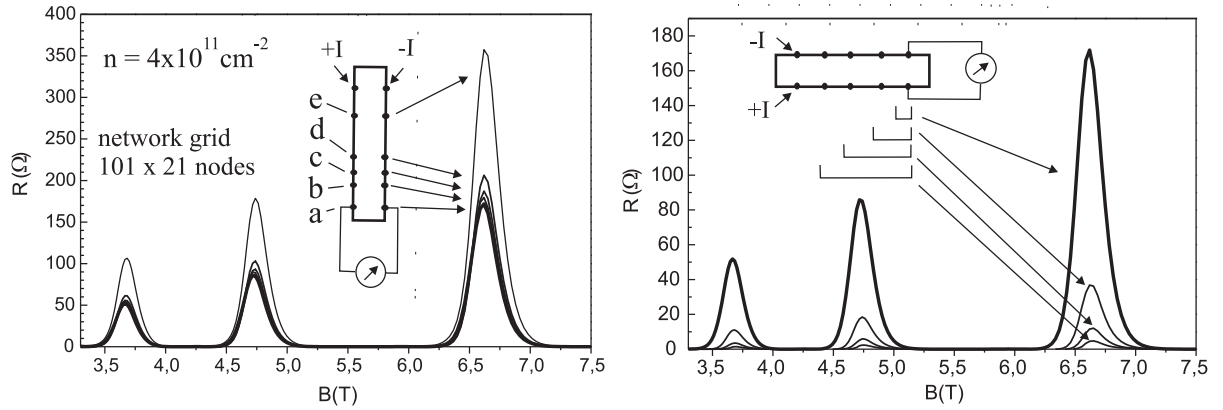


Figure 3. Left: Non-local resistance at different distance from current injection. Insert: Contact scheme of the point contact pairs with a-e marking the different positions for taking the signal. In this case only one voltage contact pair is present at a time. The contacts for current injection are marked with +I and -I. Right: Non-local resistance at fixed position, but with different number of additional unused contact pairs attached at the same time, like indicated in the insert (indicated by the square brackets)

For obtaining a better understanding of the non-local signal, we change now to the rectangular geometry with point contacts at the edges, but no contact leads. That provides more flexibility in changing conduct configurations without changing the Hall conductor as a whole and thus allowing us to compare different contact configurations more easily. The non-equilibrium is now created with a current contact pair at opposite edges near one end of the conductor and the non-local resistance is investigated for different contact configurations. On the left of Fig. 3 the dependence of the non-local resistance on the distance from current injection is demonstrated and one can see that the non-local resistance goes down with distance. On the right of Fig. 3 we show the behavior of the non-local resistance at fixed distance but with a different number of unused contact pairs between current injection and remote voltage probes. The non-local

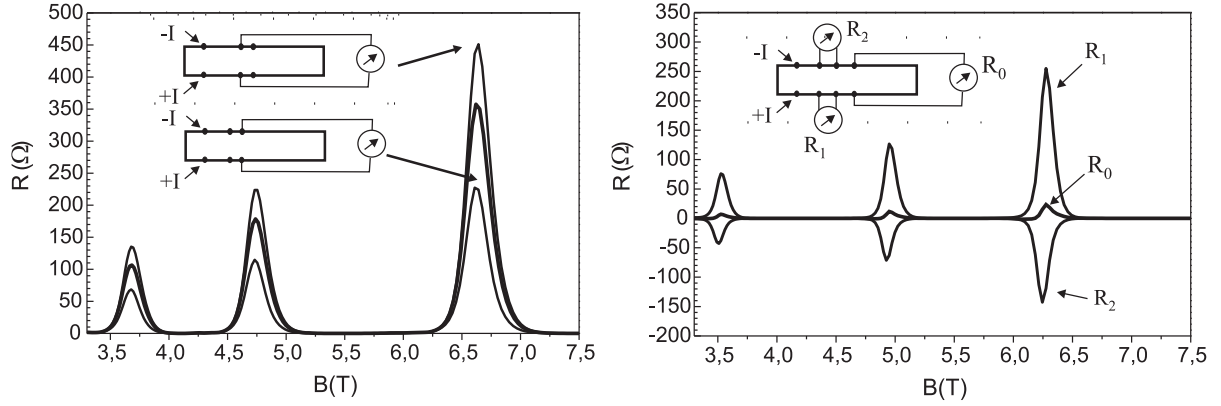


Figure 4. Left: Non-local resistance of a QH conductor taken at fixed voltage contact pair, without and with an unused contact pair, but introduced once before and once after the voltage probes. Right: Non-local resistance at 3 voltage contacts pairs, one across the Hall bar (R_0), one at the lower (R_1) and one at upper edge (R_2) like indicated in the insert.

resistance goes down with the number of unused contacts, because any additional contacts introduce additional equilibration between edge and bulk, which removes a part of the non-equilibrium already before arriving at the voltage probes. Since in our study the non-local signal is observed as a potential difference between opposite edges, this at the same time indicates an edge current that is delivered to the remote region. However, since there are no further current carrying contacts in the remote region, this edge current has to be balanced by a counter flowing bulk current for current conservation reasons.

The left side of Fig.4 shows the non-local resistance at fixed position, but comparing the case without additional contacts and the cases with an additional contact pair, but once in front and once behind the voltage probes (see insert on the left). One can clearly see, that the additional contact pair in front of the voltage probes reduces the non-local resistance as compared without additional contacts, but if the additional contacts are on the other (right) side of the voltage probes, the non-local resistance increases. This can be understood quite easily in the following way: The direction of the ECs is counter clockwise in this simulations. Therefore the lower ECs pick up the positive potential of the lower current contact and carries that all around the sample to the negative current contact, while loosing successively some of the potential due to the ongoing equilibration all along the edge and eventually present additional contacts. If there are additional contacts on the right side, they appear on the way from the voltage contact on the lower edge to the voltage contact at the upper edge, which enhances the voltage drop between these non-local voltage contacts. This increases also the non-local edge current to be delivered to the remote side, which has to pass the voltage probes. Therefore the resulting additional non-local voltage can alternatively also be roughly understood in terms of a Hall voltage of that remote edge current caused by the equilibration processes in the remote region.

In order to clarify the discussion so far, Fig.4 on the right shows the non-local resistance of the remote voltage probes like before, but now there are 2 additional longitudinal voltage contact pairs at the upper and lower edge in order to measure also the longitudinal non-local resistance. As one can see, R_0 gets almost suppressed because of the additional contact pairs, but one can also see, that in contrast to R_1 , R_2 at the upper edge is negative. This means that the voltage drop along the upper edge is opposite to that of the lower edge. This is consistent with the above discussion concerning the remote edge current, which comes up because of the equilibration process in the remote region. Since the conducting bulk channels, which are needed

for balancing the remote edge current, exist only in the transition regime between quantum Hall plateaus, such non-local signals appear only in the plateau transition regime, just like the local longitudinal resistance.

4. Summary

Using a non-equilibrium network model we have studied different non-local configurations of a quantum Hall system. We have shown that any additional voltage probes affect the results at all other contacts by introducing an additional edge-bulk equilibration. We have also demonstrated, that edge-bulk equilibration in the remote region causes a remote edge current, which has to be balanced by a bulk current. This remote edge current is mainly responsible for the non-local signal, which can be roughly understood as a type of Hall voltage of that remote edge current.

5. Acknowledgments

Financial support by the Austrian Science Foundation (FWF) Project Nr. P19353.

References

- [1] K. Ikushima, et al, Physica E **42** (4), 1034 (2010)
- [2] J. Oswald, International J. Mod. Phys. B**21**, 1424 (2007)
- [3] M. Oswald, Oswald, R.G. Mani, Phys. Rev. B**72**(3), 35334 (2005)
- [4] M. Oswald, Oswald, Phys. Rev. B**74**(15), 153315 (2006)
- [5] C. Uiberacker, C. Stecher, J. Oswald, Phys. Rev. B **80**(23), 235331 (2009)
- [6] J. Oswald, et al, JOURNAL OF LOW TEMPERATURE PHYSICS **159**, 180 (2010)
- [7] J. Oswald and M. Oswald, J. Phys. Cond. Mat. **18**, R101 (2006)
- [8] C. Sohrmann, J. Oswald, and R.A. Römer, Lecture Notes in Physics **762**, 163 (2009)